Ne pas mettre sur les listes avant le 1er novembre -

EUROPEAN ORGANIZATION FOR NUCLEAR RESEARCH

FD/HR/afm

CERN PS/87-63 (AA)

DYNAMICS OF A Z-PINCH FOR FOCUSING HIGH-ENERGY CHARGED PARTICLES

F. Dothan
Hebrew University of Jerusalem

H. Riege
European Laboratory for Particle Physics (CERN), CH-1211 Geneva 23

E. Boggasch and K. Frank
University of Erlangen-Nürnberg

Abstract

The dynamics of a linear z-pinch is studied. Through the pinched plasma column of length 270 mm and diameter up to 40 mm flows a current of maximum 400 kA; the resulting azimuthal magnetic field, spatially and temporally stable for up to 0.5 μs, shall be used as a focusing lens for a charged particle beam. The discharge current and voltage were measured, as well as the magnetic field strength at different radii. The current density as a function of radius and time was derived, and also the velocity and width of the imploding current layer. Current loops ("inductons"), excited near the maximum contraction moment, were found; they lead to a favourable amplification of the pinch current and of the magnetic field in the column. By choosing aluminium oxide as wall material and hydrogen as filling gas the formation of harmful wall currents can be avoided.

(Paper published in the Journal of Applied Physics)

Geneva, Switzerland
August 1987

Abstract

The dynamics of a linear z-pinch is studied. Through the pinched plasma column of length 270 mm and diameter up to 40 mm flows a current of maximum 400 kA; the resulting azimuthal magnetic field, spatially and temporally stable for up to 0.5 μs, shall be used as a focusing lens for a charged particle beam. The discharge current and voltage were measured, as well as the magnetic field strength at different radii. The current density as a function of radius and time was derived, and also the velocity and width of the imploding current layer. Current loops ("inductons"), excited near the maximum contraction moment, were found; they lead to a favourable amplification of the pinch current and of the magnetic field in the column. By choosing aluminium oxide as wall material and hydrogen as filling gas the formation of harmful wall currents can be avoided.

Introduction

High-energy charged particle beams can be focused by magnetic quadrupole lenses, or by a device producing an azimuthal magnetic field B. Such a field can be created by a magnetic horn[1], or by a "wire"[2] lens. A wire lens is essentially a cylindrical conductor through which flows a strong axial current of uniform density. The resulting B-field, which is linearly increasing with radius inside the conductor, leads to simultaneous focusing in all transverse directions. A wire lens is the most efficient device for focusing antiprotons ($\bar{p}$) with a large production cone, as it will be the case for $\bar{p}$ to be transferred to the future CERN ACOL ring.

In the "plasma lens" the conductor is a column of ionized gas. This gas is practically transparent for high energy particles and does not deteriorate the emittance of the beam being focused.

A plasma lens based on the z-pinch effect was designed, built, and installed in the Alternating Gradient Synchrotron at BNL in 1965[3]. In this type of plasma lens a pulse of high current flows through a partly preionized gas, producing total ionization and an imploding plasma column. The particles to be focused pass through the plasma lens near the moment when the plasma column reaches its minimum ("pinch") diameter.

The BNL plasma lens successfully focused secondary particles, but failed after only a few hours of operation. No further applications of this kind have been pursued since, until a research and development program was started at CERN in 1983[4,5]. Here the design goals are a plasma column of 40 mm diameter and 270 mm length, carrying a current of 400 kA for 0.5 μs. Radially constant current density is desirable, but deviations from linearity up to ± 10% can be accepted. Such a lens can collect antiprotons up to an angle of 0.2 rad emerging from a 3 mm diameter, 55 mm length iridium target situated 110 mm from the entry to the plasma column. The plasma lens has to have a lifetime of at least $1.5 \cdot 10^6$ pulses at a repetition rate of 0.4 Hz.

The two main objectives of plasma lens development at CERN were the achievement of the required dimensions and current density of the plasma column and of sufficient life-time of the plasma lens tube. Unfortunately the causes of failure of the BNL plasma lens were not known. Before installing a plasma lens into the ACOL target area the failure mechanisms had to be studied in the laboratory[6]. Plasma dynamics and long term behaviour are now so far under control that testing of a plasma lens in the beam is envisaged for 1988. The main differences compared to the BNL lens will be:

- hydrogen as filling gas instead of argon
- aluminium oxide as tube wall material instead of fused silica
- hollow electrodes instead of plane electrodes
- no longitudinal, stabilizing field, B_z, which would need an additional pulse generator
- 20 kJ stored pulse energy instead of 100 kJ
- shorter pulse length of 30 μs instead of 60 μs.

The stability and reproducibility of the pinch conditions will not be dealt with in detail here. Generally instabilities occur only after the first contraction phase where the pinch will be used for focusing.

Kink (m = 1) instabilities can well be observed with the two magnetic probes at fixed longitudinal position because they would lead to different signals on both probes. Balloon (m = 0) instabilities do not appear at the same longitidunal position with always the same amplitude. Hence they can be also recognized by reproducibility measure-

ments. With streak photography this has been verified on an earlier plasma lens prototype[4,6]. The results of stability measurements with magnetic probes and streak photography will be reported elsewhere.

In this paper we report results of measurements of the azimuthal magnetic field strength B(r,t) as a function of radius and time, as well as other quantities derived from B(r,t), such as current density j(r,t) as a function of time and radius, and the velocity of the imploding plasma layer. Total pinch current and voltage were also measured. The influence on these quantities of various parameters (gas type, gas density, capacitor bank voltage and wall material) will be discussed. Additional results are the appearance of current loops ("inductons")[7] and wall currents.

Z-Pinch Models

The theory of the dynamic z-pinch has been discussed since 1954. We shall here describe shortly three models that have been conceived in order to explain the phenomena in the linear pinch. The first one[8] is the "snowplow" model in which the plasma current is assumed to be confined inside an infinitely thin cylindrical shell. At the beginning, the current flows along the container wall, where the inductance of the configuration plasma-return conductor is minimum. Then, because of magnetic pressure, the shell moves towards the axis, sweeping up all particles it encounters. This model, based on momentum conservation, predicts an infinite compression on the axis. The scaling laws for the pinch time were of some practical use for a former lens prototype[4].

In the more realistic model of Miyamoto[9], a current shell of finite width is confined between a shock front and a "magnetic piston" (Fig. 1), which move radially inwards. Energy conservation is considered, in addition to momentum conservation. This "snowplow energy model" describes qualitatively the observed imploding annular current layer, the pinch radius, the time to minimum radius of the current-conducting plasma column ("pinch time"), and the subsequent oscillatory behaviour.

A further refinement of the theory is the addition of the electrical circuit equations to the plasma MHD equations[6]. The circuit

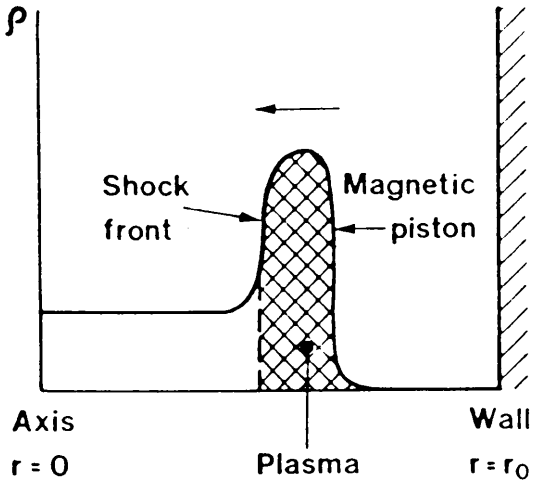

Fig. 1

Gas mass-density ρ as a function of radius at a certain time during the implosion phase of a z-pinch.

equations take into account electrical parameters (Fig. 2), including the time-varying pinch inductance L_p. Here a set of self-consistent non-linear differential equations is obtained. These equations can be solved numerically; Figure 3 shows some of the results for two different matching parameters α. α is the ratio of external circuit cycle time $\sqrt{L_0 C_0}$ divided by the propagation time of the shock front from the wall to the axis. Normalized variables are used; their definition is:

normalized pinch voltage : $v = v_p/V_0$

normalized radius : $x = r_p/r_0$

normalized current : $i = i_p \cdot \sqrt{L_0/C_0}/V_0$

normalized time : $\tau = t/\sqrt{L_0 C_0}$

v_p-pinch voltage; V_0-charging voltage of capacitor C_0; r_p-pinch radius; r_0-container radius; i_p-pinch current; L_0-parasitic inductance; t-time from current start.

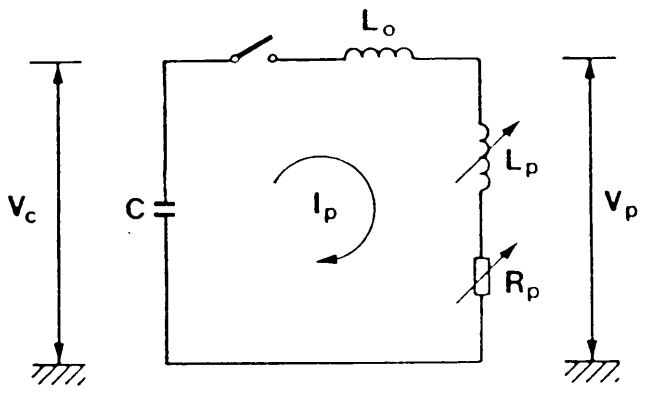

Fig. 2

Equivalent electrical circuit of the z-pinch.
C_0 - capacitance of capacitor bank;
$v_c(t)$ - capacitor voltage ($v_c(0) = V_0$);
L_0 - parasitic inductance;
$L_p(t)$ - pinch inductance;
$R_p(t)$ - pinch resistance;
$v_p(t)$ - pinch voltage;
$i_p(t)$ - circuit current.

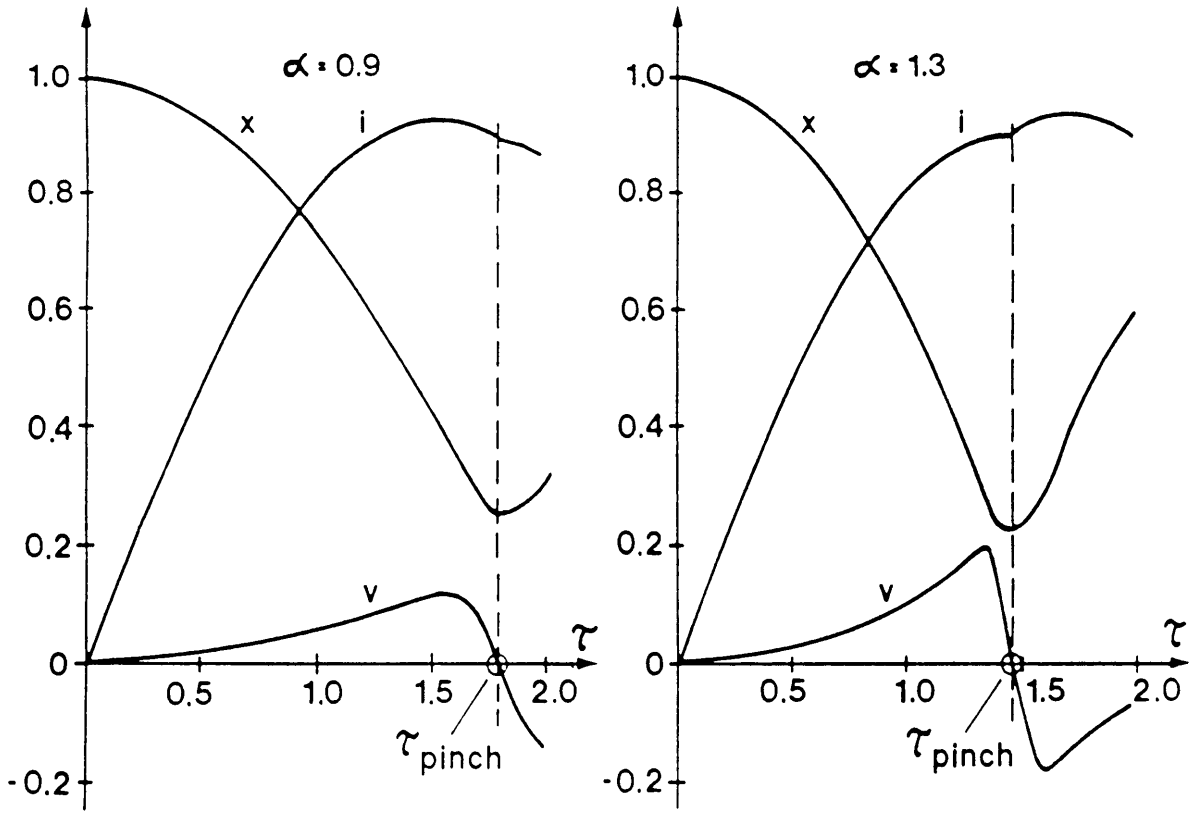

Fig. 3 - Computed pinch radius x, current i, and voltage v, as function of time τ. Normalized variables are used (see definitions in text). The parameter α is given by $\alpha = \text{const} \cdot (V_0 C_0)^{0.5}/\varrho^{0.25} \cdot r_0)$, *where* ϱ *is the initial gas density.*

The results fit the experimentally obtained values to an acceptable degree for the case of large external inductance ($L_0 \gg L_p$)[6]. The main drawback of the theory seems to result from the assumption that the gas is totally ionized at the start of the current pulse. In reality, the gas in the present experiments is only weakly ionized at the start. The energy expenditure to dissociate the gas (e.g. when using hydrogen), and to ionize it cannot be neglected and must appear in the energy balance equation. A model including shock waves, initial ohmic resistance, ionization and dissociation energy and a degree of ionization below 100% has been developed and successfully compared with the latest prototype measurements. The results will be published at a later date.

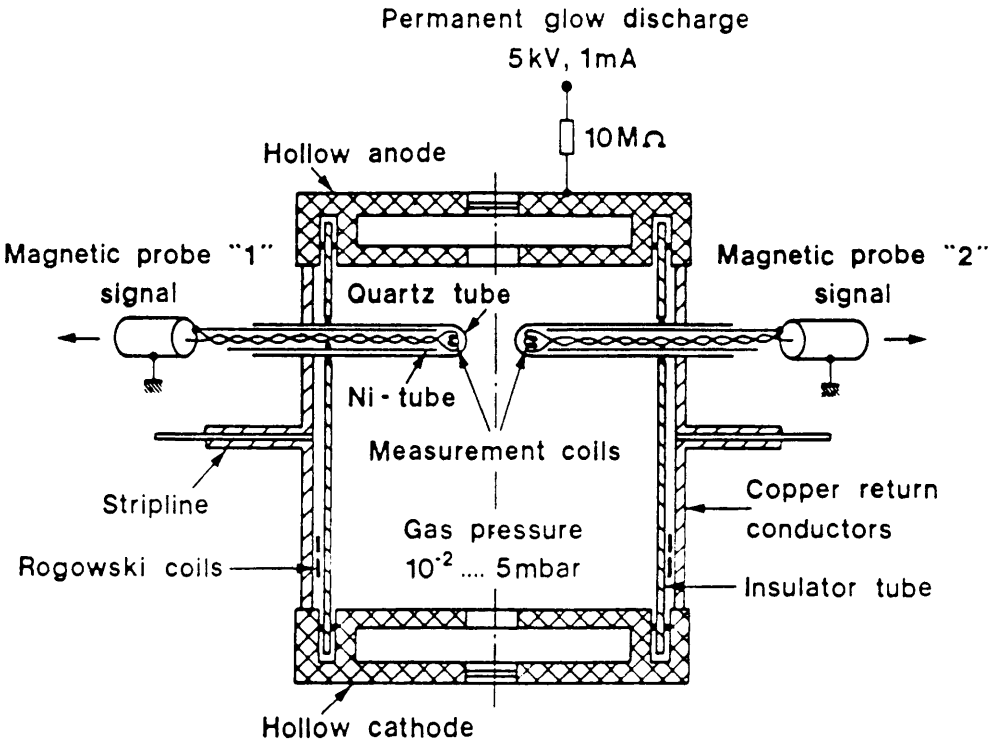

Fig. 4 - Schematic of plasma lens.

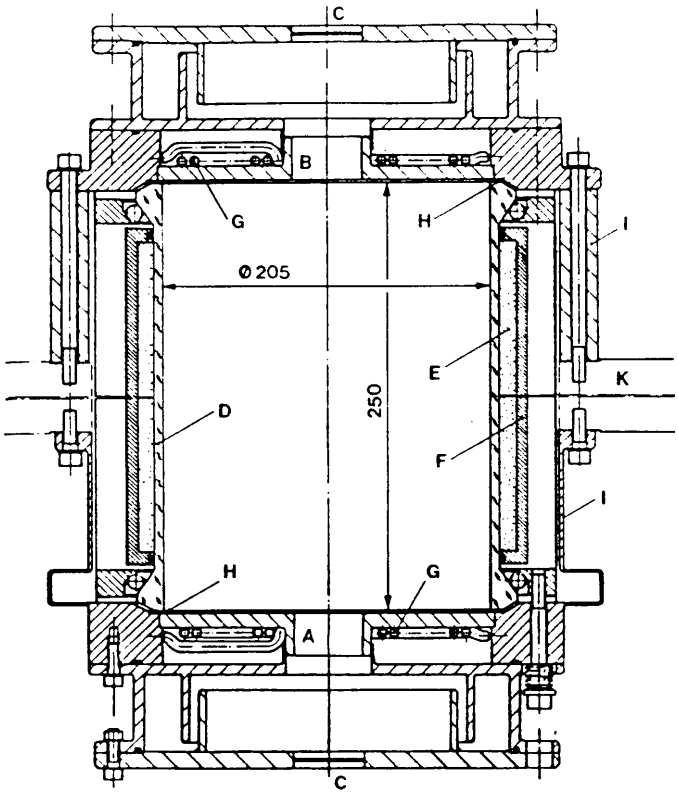

Fig. 5

Axial section of plasma lens.
A - cathode;
B - anode;
C - windows;
D - insulating tube;
E - cooling fluid;
F - jacket;
G - electrode cooling;
H - gasket;
I - current lead;
K - stripline.

Plasma Lens Prototype Design

For the use of a linear pinch in a particle accelerator hollow electrodes (Fig. 4) are favourable. Such a structure needs only thin windows in the rear electrode walls for the passage of the beam. The absorption of high-energy particles is low. These windows, which will be simultaneously exposed to the dense primary proton beam and to the hot plasma of the lens are one of the remaining technological problems which have to be solved after installation of the plasma lens in the target area. Figure 5 shows a section of one of the plasma lens prototypes which have been studied. The hollow electrode walls are made from stainless steel. Only the parts directly exposed to the plasma are made of Densimet (95% W). They are water cooled from the rear side. The insulating cylinder of 250 mm length and 200 mm inner diameter is joined to the electrodes with temperature resistant graphite seals. Different insulator tubes made from quartz, aluminium oxide, aluminium nitride and boron nitride were tested. In some experiments metallic rings or graphite rings were mounted inside the insulator. For long-term studies the exterior of the insulating cylinder had to be cooled with water or oil. Air cooling proved to be inefficient.

The Z-pinch tube is filled with hydrogen, helium or argon at pressures ranging from 10 to 1000 Pa. It is inserted symmetrically into a strip-line table which is linked to the electrodes by bolts or a metal housing as return conductors. Gas is injected via a needle valve at the cathode and pumped away at the anode.

Experimental Set-Up

The Z-pinch tube is placed in the centre of a pulse generator consisting of four identical capacitor banks of 108 μF total capacitance[10]. Each capacitor bank is linked to the central strip-line table by a 0.5 m wide sandwich strip-line containing a high-current pseudo-spark switch. In the plasma tube current amplitudes of 400 to 500 kA are obtained. By replacing the plasma tube with a low inductance short-circuit, peak currents of 800 kA have been measured. Charging voltages up to 20 kV were applied. Two parallel high-voltage regulated power supplies allow a maximum repetition rate of 0.4 Hz. The low

pressure gas in the Z-pinch tube is weakly preionized by a 5 kV/1 mA d.c. discharge.

The operation of the generator and the switches can be monitored by four Rogowski-type current pick-ups[11] incorporated into the strip-lines. Two loops for total current measurement based on the same principle are wound around the plasma tube. The signals are passively integrated with almost negligible distortion and parasitic noise. The voltage between the plasma tube electrodes is measured with commercial high-voltage probes. A photodiode, linked to the rear centre of the plasma tube cathode by a fibre optic cable, monitors the axial light output from the pinch.

The magnetic field distribution inside the tube is determined as a function of time by two electrically screened coils of 0.5 mm diameter and 0.5 mm length. Both probe coils are radially inserted into the discharge plasma through the insulator wall (Fig. 4). Quartz tubes of 4 mm diameter protect them against contact with the plasma. The coils can be moved together with their nickel screens in the radial direction. Electrostatic pick-up is negligible for this type of coil and magnetic field penetration is instantaneous, since the probes sit outside the nickel screens.

The signals are either passively integrated and available on storage oscilloscopes or they can be acquired by transient digitizers and processed in a microcomputer system.

Results and Observations

Figure 6 shows a representative oscillogram of pinch current and pinch voltage for a capacitor bank voltage (V_0) of 15 kV and a hydrogen fill of 400 Pa. Note the strong deviation of the discharge current from a sine wave form due to the variable inductance of the plasma column dominating the electrical circuit.

Figure 7 shows the measured azimuthal magnetic field B as a function of time, for different radii. The parameters here were V_0 = 12.5 kV and a hydrogen fill of 800 Pa. The imploding current wave can be discerned in the B-measurements. In the example given in Fig. 7, the velocity of the front of the current layer was about $3 \cdot 10^4$ m/s. In

radii larger than a certain minimum radius r_m (20 mm in Fig. 7) the current wave running outwards produces the second peak of B. At the radius r_m the tail of the imploding wave and the front of the reflected wave merge, producing a single peak.

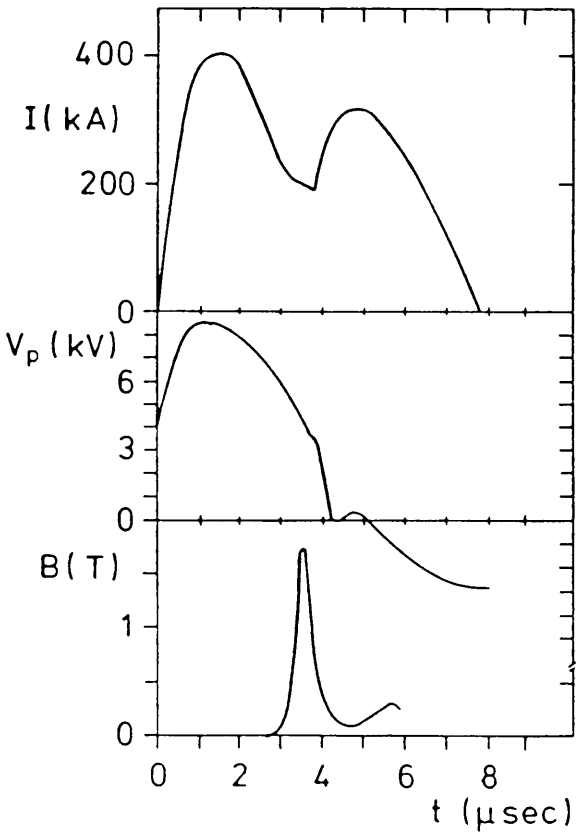

Fig. 6

Current I, pinch voltage V_p, and azimuthal magnetic field B (at radius 10 mm) as a function of time. Hydrogen 400 Pa, V_0 = 15 kV

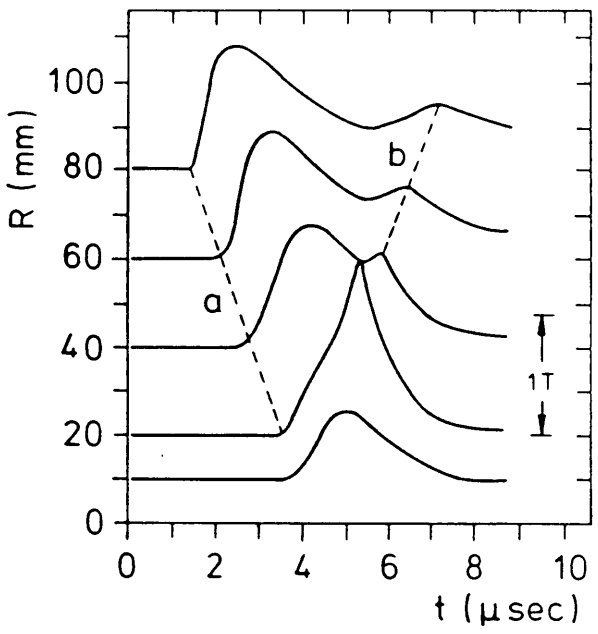

Fig. 7

Magnetic field as a function of time for different radii. Hydrogen 800 Pa; V_0 = 12.5 kV; a - front of imploding current layer; b - outward running current layer; Pinch radius - 20 mm.

Figure 8 shows the current through annular shells of 10 mm width, as a function of time. These currents were derived from magnetic field (B) measurements, for a hydrogen fill at 400 Pa and a charging voltage of 15 kV. The imploding current layer can be clearly seen, while the outward moving wave is in this case strongly damped. The substantial current near the wall (between 90 and 100 mm radius) should be noted, as well as induced current shells[12] in the opposite sense (between 30 and 90 mm radius), moving rapidly outwards near the time t_m corresponding to r_m.

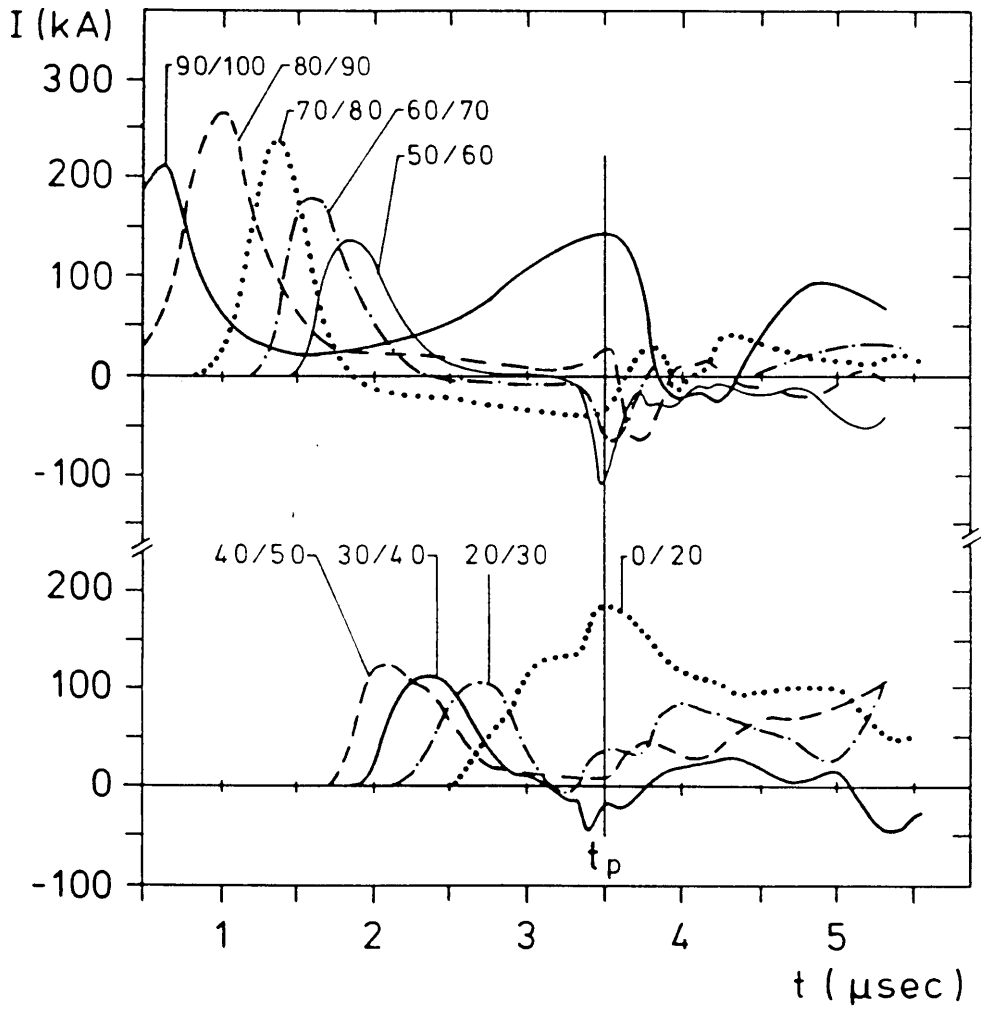

Fig. 8 - *Current between two radii (e.g. 70/80 denotes current between 70 mm and 80 mm) as a function of time from current start. Hydrogen 400 Pa, V_0 = 15 kV. Note the imploding current wave, the weaker outward running wave, the existence of wall currents (curve 90/100), and the negative currents at the pinch moment t_p.*

Figure 9 shows results of measurements of B as a function of time and radius, for a hydrogen fill of 400 Pa and a charging voltage of 10 kV. There is no magnetic field B within a radius which is a nearly linearly decreasing function of time, up to the pinch moment; this is a consequence of the imploding current layer.

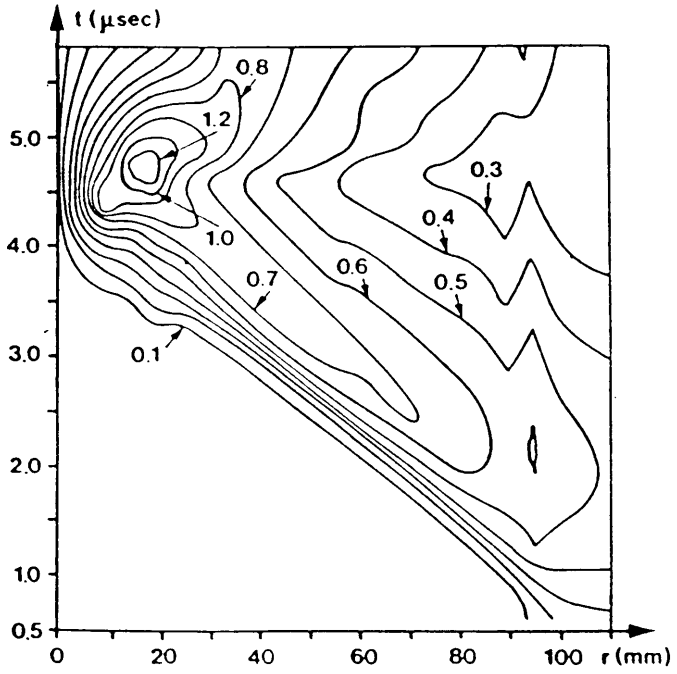

Fig. 9

Magnetic field strength B as a function of radius and time from current start; given are lines of constant B in steps of 0.1 T.
Hydrogen 400 Pa; V_0 = 10kV.

Figure 10 shows the current density as a function of radius, at the pinch moment. The parameters here were the same as for Fig. 9. The current density was derived from B measurements; the smallest radius for which B was measured here was 10 mm. The current density is approximately constant in rings 10 mm < r < 15 mm and 15 mm < r < 17 mm and equals the central current divided by the central cross section within r = 10 mm. Outside r > 17 mm it is essentially zero. The current density at radii < 10 mm could be measured only at smaller voltages[6], where it proved to be approximately constant over the pinch radius. We define the "pinch radius" as the radius r_p of a full cylinder, through which the product B·r is maximum at this voltage; B is the magnetic field measured at the radius r. The pinch time t_p is the time at which B·r is maximum. If the current density within the column is constant, then $(B \cdot r)_{max}$ is proportional to the maximum current strength within the column.

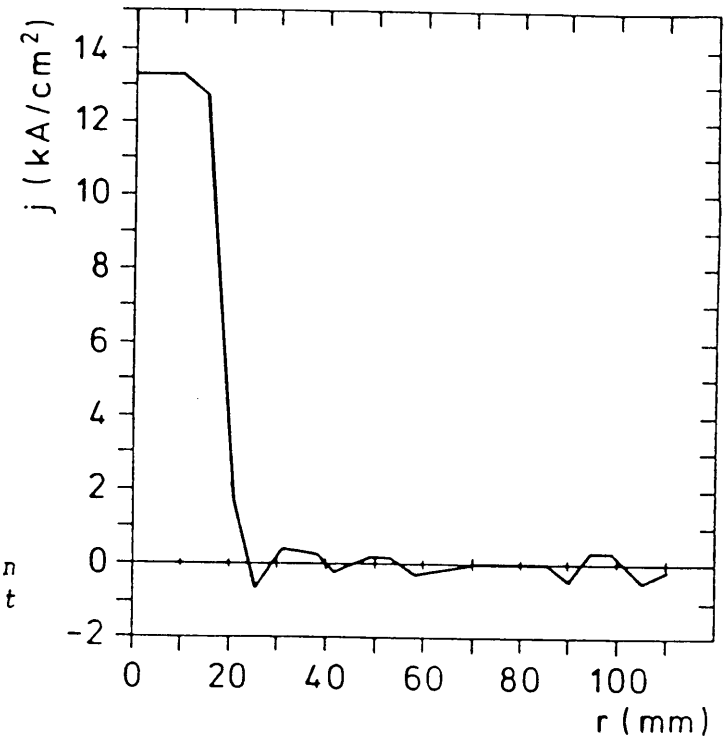

Fig. 10

Current density as a function of radius at the pinch moment (t_p = 4.7 μs). Hydrogen 400 Pa, V_0 = 10 kV.

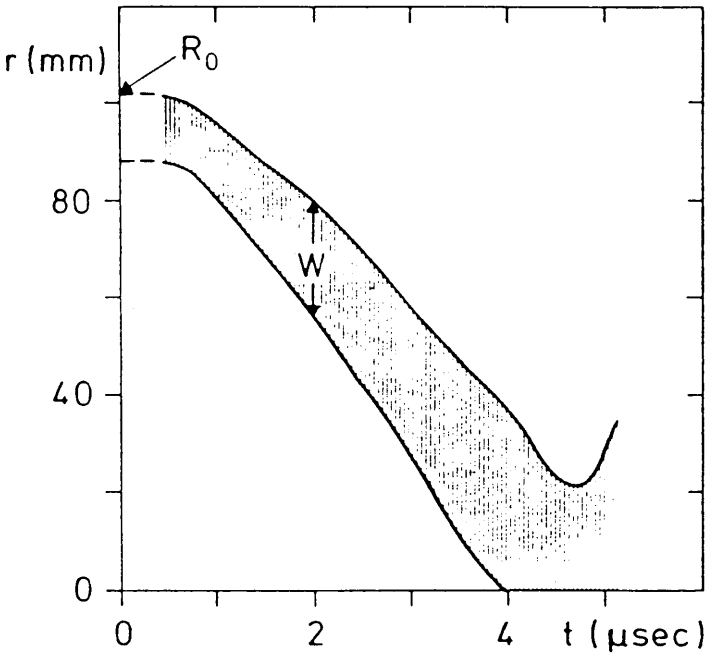

Fig. 11

Annular cylinder containing more than 90% of total current, as a function of time from current start. Hydrogen 400 Pa; V_0 = 10 kV

Figure 11 shows the width of the annular cylinder essentially containing the total discharge current for hydrogen at 400 Pa and V_0 = 10 kV. The shock front and the magnetic piston can be seen; note that the width of the current layer increases as the wave implodes. The front of the current layer proceeds with about $3 \cdot 10^4$ m/s. The finite width of the current carrying cylinder leads to a roughly constant current density distribution at the pinch moment. The pinch moment here is

t_p = 4.6 μs. Up to t_p the magnetic field is reproducible within approximately 5% from pulse to pulse. For a hydrogen fill at 400 Pa t_p decreases monotonically with increasing V_0, while r_p increases; the reason for the increase of r_p are currents in the opposite direction (seen as negative currents in Fig. 8), which amplify the current within r_p at higher V_0.

Pinch radius r_p and pinch time t_p are evaluated as functions of charging voltage for hydrogen at 400 Pa (Fig. 12). In the same figure the maximum product, $(Br)_{max}$, which is a measure of the focusing power of the plasma column, is plotted as function of charging voltage.

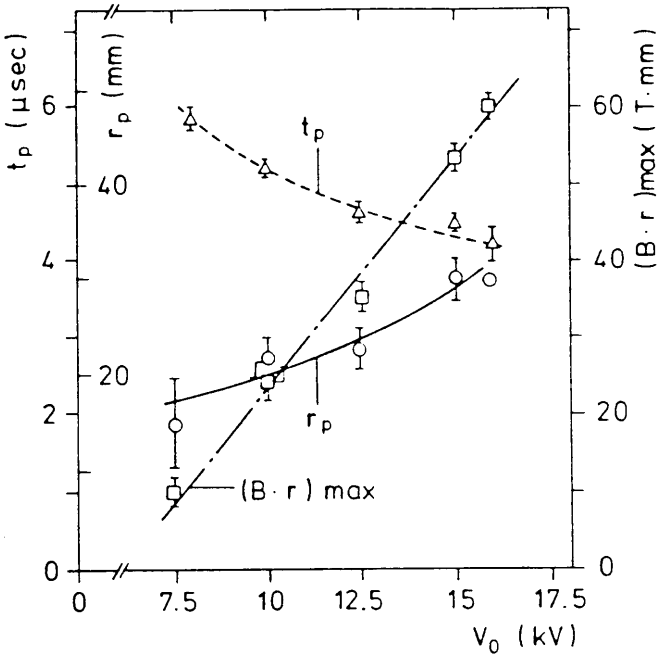

Fig 12

Pinch radius r_p, pinch time t_p, and the quality factor $(B \cdot r)_{max}$ as a function of charging voltage for hydrogen at 400 Pa.

Figure 13 shows r_p and t_p as a function of the initial hydrogen pressure, for V_0 = 15 kV. The increase of t_p with rising pressure is pronounced, while the change of r_p is slight.

Figure 14 shows the magnetic field as a function of radius at the pinch moment t_p and at a time 0.2 μs before t_p, for a hydrogen fill of 600 Pa and a charging voltage of 15 kV. The latter curve corresponds closely to a magnetic field distribution obtained from a current of 240 kA, flowing with a constant current density within a radius of 15 mm, whereas at the pinch moment a current of 280 kA is flowing within a 20 mm radius.

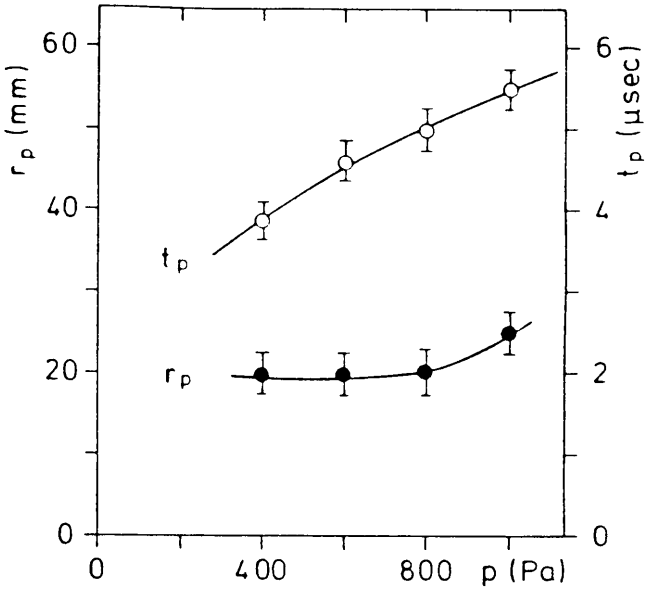

Fig. 13

Pinch radius r_p and pinch time t_p as a function of initial hydrogen pressure; charging voltage: 15 kV.

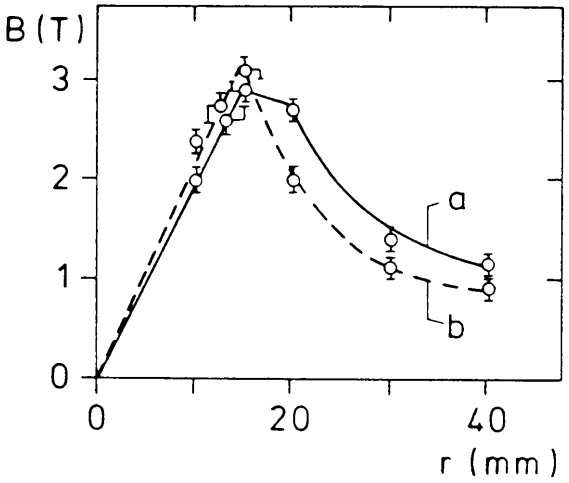

Fig. 14

Magnetic field as a function of radius at the pinch moment t_p = 4.7 µs (a) and at time t = 4.5 µs (b). Hydrogen 1000 Pa, V_0 = 15 kV.

For many combinations of gas fill and tube material wall currents were observed. For a hydrogen fill at pressures above 400 Pa and an alumina tube, wall currents exist only at the start of the pulse; subsequently, the current layer separates well from the wall and implodes towards the axis as described before. For argon/quartz or helium/quartz combinations (or hydrogen/alumina at low pressures), currents near the wall can persist for the whole duration of the pulse, and can be a substantial fraction of the total current. These wall currents are harmful because they lead to an evaporation of the wall material, i.e. erosion of the tube. Furthermore, the magnetic field in the central plasma column remains low, because wall currents bypass the pinch currents. The eroded wall material is mainly deposited on the cool electrodes and beam windows, leading to a change in performance and eventual failure of the plasma lens. A convenient measure for erosion is the effective weight loss of the insulator tube after some 10^4 to 10^5 pulses[6].

We quote here some erosion rates obtained in life-tests at 16 kV charging voltage:

Quartz/argon	35 Pa	7.5 mg/pulse
Alumina/argon	35 Pa	3.2-4.7 mg/pulse
Boron nitride/hydrogen	400 Pa	1 mg/pulse
Alumina/hydrogen	400 Pa	<0.1 mg/pulse

The electrode erosion rate is much lower than that of the insulating tube material.

The difference in performance between open electrode geometry (as in Figs. 4 and 5) and closed electrode holes was investigated. The electrode holes tend to stabilize the pinch, i.e. the scatter of the magnetic field is less for an open electrode geometry and stability lasts longer beyond the pinch moment.

It is interesting to consider the energy balance of the plasma at the pinch moment. Taking into account the plasma parameters and the measured magnetic fields, we obtain for a hydrogen fill at 400 Pa, a tube volume of $8 \cdot 10^{-3}$ m^3, a charging voltage of 15 kV and electrical circuit parameters as given before:

Total energy stored in capacitor bank	12 150 J
Ohmic losses in outer circuit	1 500 J
Dissociation energy	530 J
Ionization energy	3 280 J
Energy in magnetic field of pinch	3 000 J
Energy in magnetic field in outer circuit	500 J
Kinetic energy of plasma	1 650 J
Heat content of plasma	1 460 J
	11 920 J

In calculating the heat content of the pinched plasma, an electron temperature of 3 eV was assumed, which had been measured elsewhere under similar conditions[13]. Variation of the plasma temperature (1 to 10 eV) has little effect on this calculation of the overall energy balance. The energy balance seems satisfactory, considering uncertainties in the plasma temperature and current density distribution.

The application of a z-pinch discharge for a magnetic focusing lens requires the knowledge and mastering of the dynamic properties of the pinch. Unlike in fusion applications where high plasma density and temperature are most important, a plasma lens needs a defined magnetic field amplitude inside the pinch of defined geometry for a certain periode of time. This aim should be achieved with a minimum of energy input. It is convenient to introduce for such a lens a "quality factor" q, which is related to focusing strength. In the ideal case of a magnetic field linearly increasing with radius, the relation is:

$$\frac{S}{f} = \frac{\mu_0 e}{p} B_{max} r_p \cdot \ell = \text{const} \cdot q$$

where S is the area of the plasma column cross section, ℓ its length, f the focal length, p the particle momentum, B_{max} the maximum azimuthal field, e the elementary charge, and $q = B_{max} \cdot r_p$. The "pinch radius" r_p is defined as the radius of the column for which q is maximum; in the case of constant current density this is equivalent to the maximum current in the column. A plasma lens with the characteristics required for the CERN ACOL target has to reach q = 80 Tmm and to maintain this value over 0.5 μs. With 17 kV charging voltage at 600 Pa hydrogen pressure a quality factor of only 10% less than the design value was obtained. Full focusing strength will be reached at 19 kV (Fig. 12).

The reason for reaching a high quality factor in spite of the low total current which flows at the pinch moment is the strong amplification of the field inside the pinched plasma column by the "inductons". These current loops, which are induced as a law of nature in all pinch configurations and gases we have studied, may reach an intensity which equals the unamplified pinch current. Hence, there is a shift of magnetic energy from the external magnetic field towards the internal magnetic field energy which, in certain cases, is amplified by up to a factor four. Nevertheless, to produce 1.1 kJ internal magnetic pinch energy, almost 20 kJ stored energy are required corresponding to 19 kV charging voltage in the test pulse generator.

Most of the experiments were performed with a current rise rate of the order of 5×10^{11} A/s. Not only the energy balance is favoured by

slower current rise times, but also the pinch duration during which the magnetic field properties should stay constant can be extended to 0.5 μs. A doubling of the generator cycle time and hence a four times greater storage capacity at half the present voltage is needed. Measurements of the inducton excitation at lower voltages and current rise time show rather an increase of pinch amplification compared with faster current rise. Hence, one can expect equal or better pinch amplification at a lower current rise rate. Another advantage at lower di/dt is the improvement of spatial and temporal stability of the pinch.

Conclusions

The imploding current layer predicted qualitatively by the snowplow energy model has been observed in our experiments. The pinch time t_p as a function of charging voltage V_0 corresponds closely to that given by the theory (t_p = const : $V^{-0.5}$). The dependence of t_p on the initial gas pressure p_0 is different from that predicted, i.e. we obtained from our measurements t_p = const · $p_0^{0.38}$, as compared to the predicted t_p = const · $p_0^{0.25}$.

Considering phenomena in a pinched discharge at gas pressures and currents investigated by us, the main drawbacks of existing dynamic pinch theories seem to be the following.

* Assumption that the gas is initially ionized; in reality the gas ionization and implosion are concurrent. Dissociation has to be taken into account for a molecular gas. The energy required for dissociation and ionization can be a substantial part of the stored energy.

* Neglect of wall currents. For certain combinations of gas and wall material the wall current can be a large part of the total discharge current. The current in the pinched column is then correspondingly reduced.

* Neglect of negative currents. Current loops ("inductons"), consisting partly of current in a direction opposite to the main current, are <u>always</u> induced by the change of the magnetic flux of the imploding-exploding current column. This current does not

appear in the measurement of the total current, but can be clearly deduced from magnetic probe measurements (e.g. see Fig. 8). In practice the highest negative currents appear outside the pinched plasma column when it starts to expand, following the first contraction. At the same time the current within the pinched column is amplified, thus increasing the quality factor $q = B \cdot r$ (proportional to the focusing power). The existence of negative currents indicates the presence of a conducting plasma outside the pinched column; evidently not all the gas is swept up by the magnetic piston.

The present results on the dense z-pinch, in conditions investigated by us, show that it is possible to use the pinched plasma column as a focusing lens for charged particles. The principal features of such a lens are: negligible absorption of particles, a manageable plasma dynamics, and prevention of plasma-wall interactions by choice of appropriate gas/wall-material combinations.

Acknowledgements

The authors are very much indebted to M. van Gulik and Y. Thébault for their help in preparing and performing the measurements.

References

1. S. van der Meer, CERN 61-7 (1961).

2. B.B. Bayanov, G.I. Budker, G.S. Villeval'd, T.S. Vsevolozhskaya, L.L. Danilov, V.N. Karasyuk, G.I. Sil'vestrov, V.A. Tayurskiy and A.D. Chernyakin, Proceedings of the Xth International Conference on High-Energy Acclerators, Protvino, July 1977, Vol. II, pp. 103-109. Translated, May 1984, by AD-EX Translations International, USA.

3. E.B. Forsyth, L.M. Lederman, J. Sunderland, IEEE Trans. Nucl. Sci. 12, (1965), 872.

4. J. Christiansen, K. Frank, H. Riege and R. Seeböck, CERN/PS/84-10 (AA), (1984).

5. L. De Menna, G. Miano, B. Autin, E. Boggasch, K. Frank, and H. Riege, CERN/PS/84-13 (AA), (1984).

6. B. Autin, H. Riege, E. Boggasch, K. Frank, L. De Menna and G. Miano, IEEE Trans. on Plasma Science, PS-15, NO. 2, (1987), 226. Special Issue on Plasma-Based High-Energy Accelerators.

7. I.Y. Butov and Y.V. Matveev, Sov. Phys. JETP 54, (1981), 299.

8. M. Rosenbluth, H. Garwin and A. Rosenbluth, Los Alamos Scientific Lab. Rep. LA-1850, (1954).

9. T. Miyamoto, Nucl. Fusion, 3 (1984), 337.

10. E. Boggasch, V. Brückner and H. Riege, Proc. of the 5th IEEE Pulsed Power Conf., P.J. Turchi and M.F. Rose, Editors, published by the IEEE, Arlington, (1985), 820.

11. E. Boggasch and R. Grüb, CERN/PS/86-25 (AA), (1986).

12. I.R. Jones and C. Silawatshananai, Plasma Physics, Vol. 22, (1980), 501.

13. K.H. Finken, G. Bertschinger, S. Maurmann and H.J. Kunze, J. Quant, Spectrosc. Radiat. Transf., 20, (1978), 467.